

## Detection of coastal landforms in a deltaic area using a multi-scale object-based classification method

Tapas R. Martha<sup>1,\*</sup>, A. Mohan Vamsee<sup>2</sup>,  
Vikas Tripathi<sup>3</sup> and K. Vinod Kumar<sup>1</sup>

<sup>1</sup>Geosciences Group, National Remote Sensing Centre,  
Indian Space Research Organization, Hyderabad 500 037, India

<sup>2</sup>Department of Geo-engineering,  
Andhra University College of Engineering (A),  
Vishakhapatnam 530 003, India

<sup>3</sup>Department of Physical Sciences,  
Mahatma Gandhi Chittrakoot Gramodaya Vishwavidyalaya,  
Chittrakoot 485 780, India

**Coastal landforms play an important role in protecting deltaic areas from erosion due to the action of waves. However, landforms in the deltas are dynamic and vulnerable to changes due to the effect of natural disasters like floods and cyclones. Automatic detection of dynamic landforms from satellite data can provide important inputs for effective coastal zone management. In this study, we developed an Object-Based Image Analysis (OBIA) technique to identify and map landforms in the Krishna delta, east coast of India using Resourcesat-2 LISS-IV multispectral image (5.8 m) and digital elevation model (DEM) (4 m). Since landforms are represented at multiple scales, the plateau objective function method was used to select appropriate scales during multiresolution segmentation. Knowledge-based rules in OBIA, using the parameters tone, texture, shape and context derived from satellite images and height from DEM were developed for classification of landforms. A total of 11 landforms (beach, beach ridge, swale, tidal creek, marsh, spit, barrier bar, mangrove, natural levee, channel island and channel bar) were mapped using this approach. High detection accuracy of these landforms indicates that the method developed has the potential for geomorphological mapping of dynamic landforms in low lying deltaic areas.**

**Keywords:** Beach, cyclone, DEM, image segmentation, mangrove, OBIA, Resourcesat-2.

COASTAL zone is important for the high productivity of its ecosystem, concentration of population and exploitation of renewable and nonrenewable natural resources. It occupies more than 10% of the Earth's surface, and about 40% of the world's population lives within 100 km from the coast. In India, about 35% of the population resides within 100 km of the coastline<sup>1</sup>. Erosion, accretion, inundation due to sea level rise, storm surge, shifting of shoreline caused by natural (e.g. floods and cyclones) or anthropogenic forces such as construction of artificial

structures, port and harbour modify the coastal and fluvial landforms and its environment constantly<sup>2</sup>. Therefore, dynamic landforms need to be monitored periodically and maintained suitably for the sustainability of human life and ecosystem. For this purpose, we need to update the coastal geomorphology to develop efficient land management strategies.

Coastal landforms can be monitored appropriately using remote sensing data than the conventional methods<sup>3,4</sup>. With increasing availability of high resolution spectral and spatial satellite images, remote sensing is delivering data on landform location and extent<sup>5-7</sup>. In developing countries with increasing population and expansion of infrastructure, geomorphological map provides key inputs for mapping of natural resources and assessment of natural hazards<sup>8</sup>. Geomorphological mapping is done efficiently with the help of remote sensing, geospatial technologies and GIS on a national scale<sup>9-12</sup>. However, in deltaic lowland environment, landform detection from satellite image is complicated because of subdued relief and lack of spectral characteristics of landforms due to land cover changes, offering a challenge to draw clear cut boundaries of terrain forms, such as river water line, coastline and associated landforms<sup>13</sup>.

Object-Based Image Analysis (OBIA) using satellite image and DEM has shown promising result for landform classification<sup>14-17</sup>. According to a widely accepted definition of OBIA proposed by Hay and Castilla<sup>18</sup>, 'OBIA is a sub-discipline of GIS devoted to partitioning of remote sensing imagery into meaningful image objects, and assessing their characteristics through spatial, spectral and temporal scale'. An object can be defined as a group of pixels with homogeneous spectral and spatial characteristics. In this study, OBIA was used for the detection of landforms in a low lying deltaic area since objects appropriately represent the surface forms in a manner we visualize them in the terrain. It is also easy to use additional data (e.g. elevation, base map and attribute data) in this approach to increase the classification accuracy. Moreover, the terrain being continuous in nature, per-pixel methods of image classification will have several limitations in handling landforms, e.g. per-pixel classes do not relate to individual landform elements and yield scattered classes across the scene<sup>19</sup>. Object-based classification approach also allows us to explore all aspects of remote sensing, including spectral, spatial, contextual, textural and temporal properties for feature extraction. Although automatic landform mapping using OBIA has been attempted<sup>14-17</sup> in mountainous high lands, to the best of our knowledge, there has been no effort to automatically map landforms in deltaic low land areas. In this study, we developed an object-based multi-scale approach to classify landforms in the Krishna delta in east coast of India with knowledge-based rules using high resolution satellite data and DEM. Landforms represented at different scales in low lying deltaic areas were

\*For correspondence. (e-mail: tapas\_martha@nrs.gov.in)

detected using the multi-scale knowledge-based approach.

The Krishna River originates from the Western Ghats (mountains) near Mahabaleshwar in western India and meets the Bay of Bengal in east coast of India after flowing ~1300 km (Figure 1). The river forms a deltaic plain before its four distributaries debauch into the Bay of Bengal. The first distributary of the river starts near Avani-gadda but the three main distributaries of the modern river splits into the Golumuttapaya, Nadimieru and the Main channel<sup>20</sup>. Krishna river basin shares a common border with that of the Godavari River basin in the north. About 75% of the Krishna river basin is under a semi-arid climate. The annual rainfall in the delta is 910 mm with precipitation mainly from June to October<sup>21</sup>. Reduced inflow of water in the Krishna River to the delta because of the construction of dams and reservoirs decreased the sediment supply, which resulted in delta retreat<sup>22</sup>.

The main geomorphic features in the Krishna delta are ancient channels, ancient beach ridges and mangrove swamps. Mangrove swamps occur in abundance in the intertidal mudflats on both sides of the creeks. Encroachment in mangrove area for agriculture, aquaculture and industrial expansion is making an adverse impact on the ecosystem of this area. Numerous ancient channels are present in the Krishna delta on either side of the present river course indicating the earlier courses of the river.

A knowledge-based classification using an object-based technique was developed to identify landforms from the satellite image and DEM. The knowledge of satellite image interpretation for landform mapping was translated into a set of rules using spectral, spatial, elevation and contextual criteria of objects. Landforms and their characteristic features used in the classification are given in Table 1.

Multispectral data acquired on 24 May 2013 by the LISS-IV sensor onboard Resourcesat-2 satellite were

used for image segmentation and to derive the spectral characteristics of landforms such as NDVI and brightness. LISS-IV has 5.8 m spatial resolution and three spectral bands, viz. green (0.52–0.59  $\mu\text{m}$ ), red (0.62–0.68  $\mu\text{m}$ ) and near infra-red (0.76–0.86  $\mu\text{m}$ ). DEM created from Lidar data with 4 m grid size was used in the landform classification. The vertical RMSE of the DEM is 35 cm.

Image segmentation constitutes the initial part of the analysis. In this study, we have applied multiresolution segmentation (MRS) implemented in the eCognition software. MRS is a bottom-up region merging technique in which segments/objects are created using a scale parameter (for size of the object) and homogeneity criteria such as shape parameter (for geometry of the object) and colour parameter (for spectral attributes of the object)<sup>23</sup>. In eCognition software, there is scope to control the shape of the object using the parameters (smoothness and compactness). While scale parameter can be a whole number with any value, shape and colour parameters are assigned with weights between 0 and 1 and the sum of homogeneity criteria should be 1. Similarly, the two parameters (smoothness and compactness) are assigned with weights between 0 and 1 and the sum of both the parameter weights should be 1. MRS is capable of creating objects that can represent natural boundaries and thus has been applied in various types of feature detection such as hills and valleys, landslides and craters<sup>24,25</sup>. MRS was performed on Resourcesat-2 LISS-IV multispectral image. Weights of shape and colour parameters were retained as 0.1 and 0.9 respectively. Compactness and smoothness were assigned equal weights (0.5). The scale parameter determines the maximum heterogeneity allowed during segmentation, and has a direct influence on the size of the objects to be obtained. Landforms in nature occur in different shapes and sizes. Therefore, a single scale parameter in MRS will not help in achieving best classification accuracy<sup>26</sup>. Hence, we derived optimal scales in the image using the plateau objective function (POF) proposed by Martha *et al.*<sup>26</sup> and performed multi-scale classification of landforms according to their sizes.

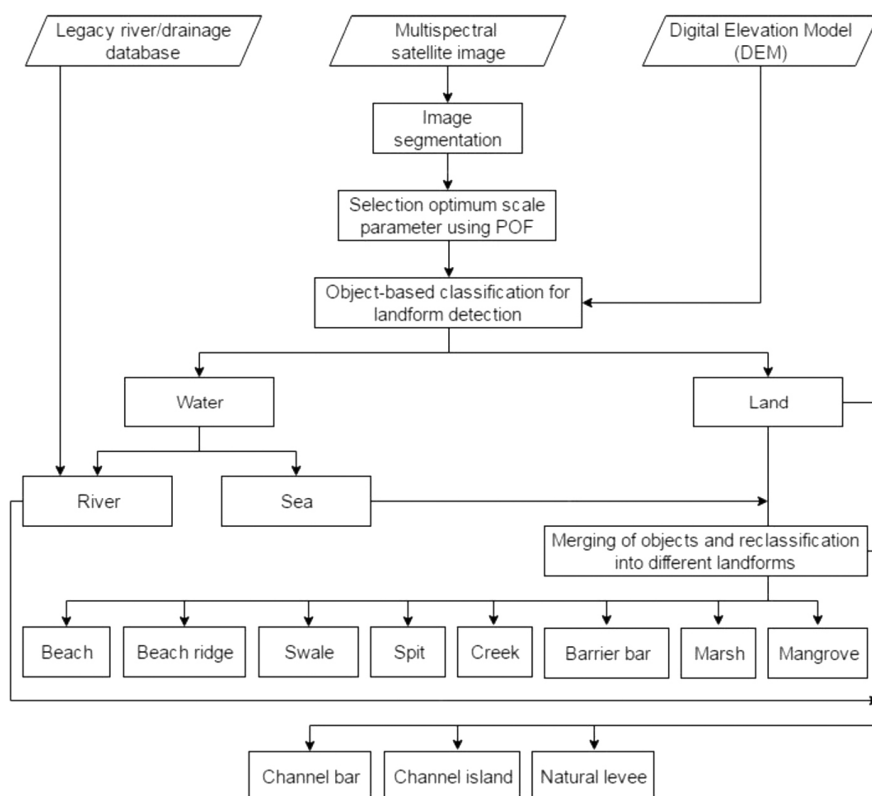
To delineate various types of landforms in coastal areas, the first step is to classify water and land from the satellite images. The next step is to classify water into seas and rivers. Legacy river vector database available with NRSC was used during the image segmentation in eCognition. Using the 'read thematic attribute' algorithm available in the eCognition software, attribute codes of the river vector layer were assigned to objects, and subsequently classified as rivers. Once the water was classified as rivers, the objects were merged to create a single river object, which will help in the identification of fluvial landforms with an adjacency condition in subsequent steps. Merging of the objects and reclassification is an important part of OBIA. Objects, once classified into a particular class, can be merged into a single object for further segmentation using other scale parameters



Figure 1. Location map of the study area in Krishna delta.

**Table 1.** Characterization of landforms in deltaic areas

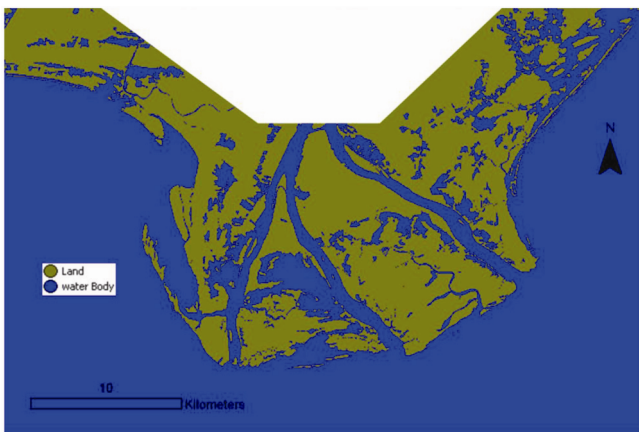
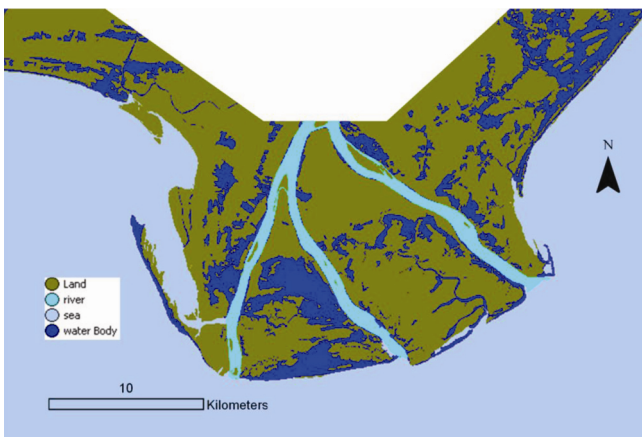
Landform	Definition	Spectral, spatial, elevation and contextual characteristics
Barrier bar	These are bars located at the mouth of the river and do not have land connection. They shelter the land from direct wave action and mostly consist of sand deposit.	Land enclosed by sea with high brightness.
Beach	The deposition of sand by sea waves along the coast.	Narrow land having high brightness and adjacent to the sea.
Beach ridge	A low, essentially continuous beach ridge of dune material heaped up by the action of waves and currents on the backshore of a beach.	Land near the sea shore and having higher elevation from the vicinity.
Marsh	A type of shallow wetland that is dominated by herbaceous instead of woody plants and often found at the edge of lakes and streams.	Water body near the sea and lakes have higher brightness than sea and lakes.
Mangrove	Trees are grown in the presence of brackish water.	Land with very high normalized difference vegetation index (NDVI) and near the sea.
Spit	Found in an irregular coastline where sediment availability and wave power allow a constructional smoothing of the coastline.	Most part of the land is enclosed by the sea but is attached to the mainland.
Swale	These are open linear depressions more common near the shoreline and parallel to the beach ridge.	Land having medium brightness and near the ridge with less elevation.
Tidal creek network	A network of natural stream of water, smaller than a river but longer than a creek.	Channel having high asymmetrical shape and near the shore.
Channel bar	An elongate deposit of sand and gravel located in the course of a stream.	Land with high brightness and bounded by the river.
Channel island	A channel bar which is stabilized with vegetation growth in the course of a stream.	Land with medium NDVI and bounded by the river.
Natural levee	Formed due to deposition from overbank flooding and acts as a barrier of water during normal flow of river.	Land near the river and have higher elevation from surrounding with high asymmetrical shape.



**Figure 2.** Flowchart for the classification of coastal and fluvial landforms.

**Table 2.** Object properties and their thresholds used in landform classification

Landform	Object threshold	Object property
Barrier bar	Mean brightness of green band is between 131 and 154 and $-0.072 < \text{NDVI} < -0.03$	Spectral
Beach	Mean brightness of red band is between 170 and 200 and distance to sea = 0 m	Spectral and contextual
Beach ridge	Mean DTM $\geq 0.56$ m, distance to sea $\leq 6$ km	Spectral, height and contextual
Marsh	Asymmetry $\geq 0.73$ and relative border to mangrove $> 0.4$	Shape and contextual
Mangrove	NDVI $> 0.15$ and distance to sea $\leq 6.5$ km	Spectral and contextual
Spit	Area $> 0.55$ sq. km, relative border to land $> 0.27$ and relative border to sea $> 0.41$	Shape, size and contextual
Swale	Brightness is between 140 and 165, distance to beach ridge $\leq 450$ m	Spectral and contextual
Tidal creek network	Brightness $\geq 122$ and NDVI $\leq -0.025$	Spectral
Channel bar	Relative border to river $> 0.74$ , NDVI $\leq 0.1$	Spectral and contextual
Channel island	Relative border to river $> 0.74$ , NDVI $> 0.1$	Spectral and contextual
Levee/natural levee	Asymmetry $\geq 0.96$ , mean DTM $\geq 0.59$ m, distance to river $\leq 1$ km	Shape, height and contextual

**Figure 3.** Land and water classification from satellite images using OBIA.**Figure 4.** Seas and rivers classified from satellite image using OBIA.

selected by POF and can also be classified into another class using additional criteria (refer figure 8 of Martha *et al.*<sup>26</sup>). This also helps in classifying landforms corresponding to their sizes. Rules based on knowledge were created using characters of landforms explained in Table 1 and classification of image was performed using object properties such as NDVI, brightness, area, asymmetry,

height, distance and relative border with a class. Flowchart for classification of landforms is given in Figure 2.

Multiple optimal scale parameters (e.g. 40, 80, 250, 290 and 330) obtained through POF were used for classification of landforms. Resourcesat-2 LISS-IV image was segmented with a scale parameter of 40. The objects having mean NIR value  $\leq 150$  and NDVI  $\leq 0.06$  were classified as water and remaining objects were assigned the land class (Figure 3).

In order to classify the sea, water class was merged and segmented again with a large optimal scale parameter, i.e. 330. This helped to create large homogeneous objects corresponding to deep water in open sea and separate small shallow inland water objects corresponding to aquaculture and marsh. Once the sea was classified using an object area threshold ( $>250,000$  sq. m), the remaining water objects were labelled as shallow water, mostly part of inland water (Figure 4).

Land was classified into various landform categories using spectral, shape, contextual and morphometric parameters derived from satellite images and DEM. Object properties and thresholds (determined through manual inspection of the image) used in classification of fluvial and coastal landforms in the Krishna delta are given in Table 2.

Fluvial landforms such as channel bars and channel islands are enclosed by the river. Therefore, we merged the land objects and used relative border of land to river as a class criteria to identify channel bars using thresholds given in Table 2. While channel bars are dynamic landforms and is exposed with a sand layer on the top, channel islands are mostly stable features with the growth of vegetation. Therefore, we used NDVI as additional criteria to separate channel islands from channel bars. Figure 5 shows the channel island mapped using OBIA and its comparison with the reference map.

To classify natural levees, the land class was merged and resegmented with a scale parameter of 80, because levees are easily identifiable as a single object with this scale parameter. Natural levees are elongated and occur adjacent to the river. Therefore, we considered the shape

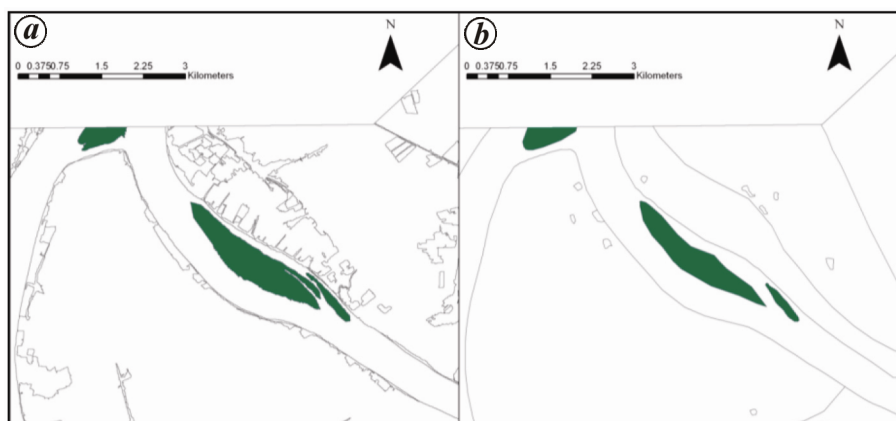


**Figure 5.** Channel island (a) mapped by OBIA and channel island (b) in the reference map.

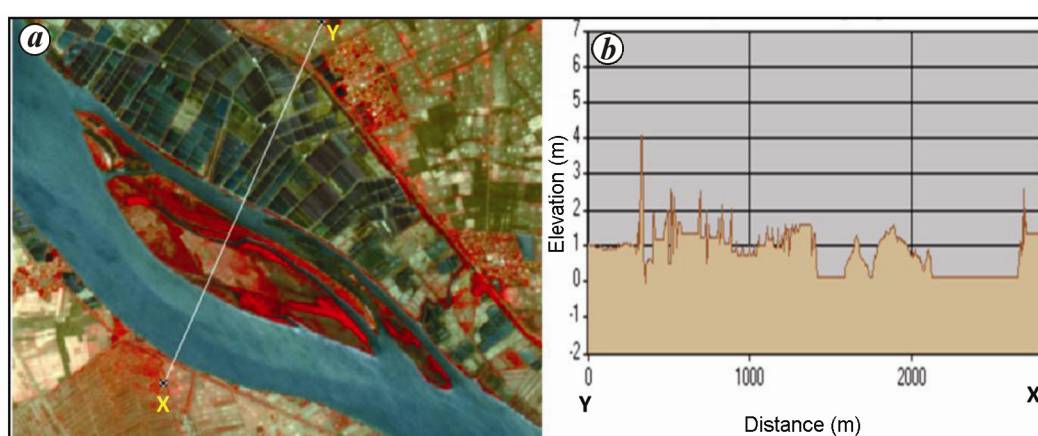


**Figure 6.** Resourcessat-2 LISS-IV image (a) showing channels island and natural levee and elevation profile of channel island and natural levee derived from DEM (b).

parameter (e.g. asymmetry of the object) and contextual parameter (e.g. distance from river) as the criteria to identify natural levees (Figure 6). The thresholds considered for the identification of landforms are given in Table 2.

Eight types of coastal landforms were mapped using OBIA in this study. Beach was classified from land objects using criteria such as high mean brightness of red layer and adjacent to the sea. Barrier bars were classified as sea since they are not segmented as individual objects (i.e. under segmentation) with a scale parameter of 330, which was used for classification of the sea. Hence, sea class objects were merged and the sea was segmented again with a scale parameter of 250 to create small size objects that can represent barrier bars. Subsequently, barrier bars were classified using mean brightness of the green band and NDVI criteria.

Beach ridges and swales are elevated and depressed landforms respectively, and are found adjacent to each other in coastal plains. They represent the position of palaestrand lines. Beach ridges are linear and elevated lands from the surrounding area and therefore, support

human settlements, roads and railway lines. As the elevation of beach ridges and swales varies within few meters, an accurate high resolution DEM is required for their classification (Figure 7). In this study, ridge and swale were classified from the land class using elevation criteria (Figure 8). Other threshold conditions used in classification of beach ridges and swales are mentioned in Table 2.

Mangrove/mangrove swamp is a typical landform, which exists only in coastal regions due to the availability of brackish water. To identify mangroves, the land objects were merged and land was resegmented using scale parameter 290. High NDVI and proximity to sea was used as the criteria to classify these landforms (Figure 9).

Creek and marsh were classified from the shallow water by merging objects and resegmenting the shallow water with scale parameters 250 and 290 respectively, and by using criteria such as asymmetry, border relation to mangrove, brightness and NDVI (Table 2). The landform map of the Krishna delta created using OBIA is shown in Figure 10.

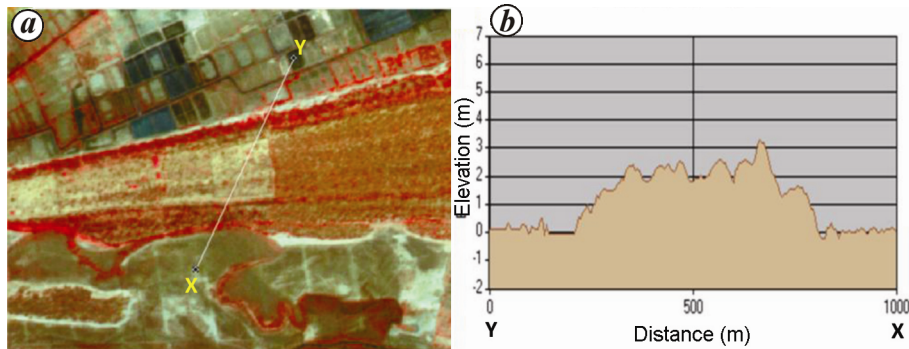


**Figure 7.** *a*, Resourcesat-2 LISS-IV image showing a beach ridge; *b*, Elevation profile across the beach ridge derived from the high resolution DEM.

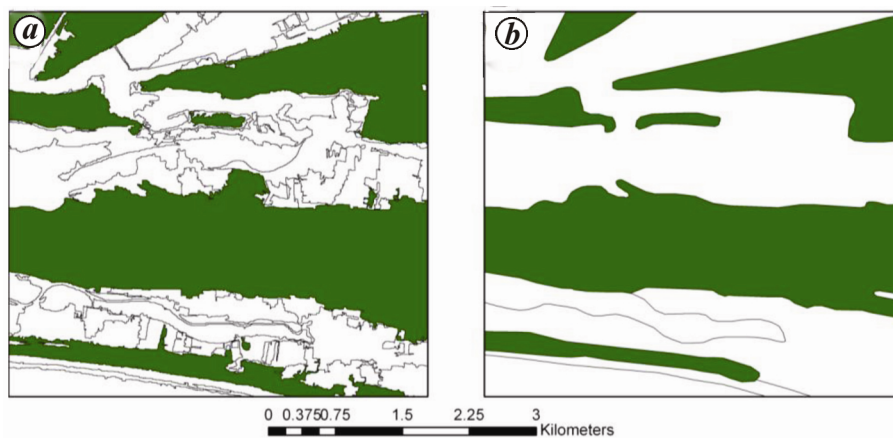


**Figure 8.** *a*, Classified map of beach ridges; *b*, Reference map of beach ridges.

We have classified 11 landforms namely barrier bar, channel bar, beach, beach ridge, creek, mangrove, natural levee, swale, marsh, channel island and spit using satellite images and DEM. Although spectrally similar, usage of contextual criteria for classifying seas and rivers helped to separate channel bars and channel islands from barrier bars. Multiple optimal scale parameters helped to identify landforms of different sizes. For example, barrier bar which could not be classified at scale parameter 330, was successfully classified with scale parameter 250. Merging objects and resegmentation proved to be useful in classification of landforms in a multi-scale approach, especially when sizes of landforms are different.

Accuracy assessment determines the quality of information derived from remote sensing data and efficacy of the developed classification method. Its purpose is to identify and measure mapping errors with respect to reference data. Geomorphological map of the Krishna delta using satellite image interpretation and field verification was used as reference data for assessing accuracy of landforms detected by OBIA technique<sup>27</sup>. The performance of the multi-scale classification method for landform mapping was measured using detection percentage, quality percentage and branching factor metrics<sup>28</sup>.

$$\text{Detection percentage} = 100 \times \left( \frac{\text{TP}}{\text{TP} + \text{FN}} \right), \quad (1)$$

$$\text{Quality percentage} = 100 \times \left( \frac{\text{TP}}{\text{TP} + \text{FP} + \text{FN}} \right), \quad (2)$$

$$\text{Branching factor} = \left( \frac{\text{FP}}{\text{TP}} \right). \quad (3)$$

True positive (TP) is the detection of actual landform, false positive (FP) is the detection of not-actual landform and false negative (FN) is non-detection of actual landform. Detection percentage can be considered as a measure of the performance of landform detection algorithm, quality percentage as an overall measure of algorithm performance and branching factor as a measure of false-detection performance<sup>25</sup>. Area of landforms was compared to calculate the accuracy figures (Table 3).

The highest and the lowest classification accuracies were obtained for barrier bar and beach respectively (Table 3). The low classification accuracy of beaches is due to wave breaks near sea shores resulting in nonsegmentation of narrow beaches from the satellite images. Detection

**Table 3.** Accuracy of landforms detected using OBIA

Landforms	TP (sq. km)	FP (sq. km)	FN (sq. km)	Detection (%)	Quality (%)	Branching factor
Barrier bar	1.2	0.0	0.0	100.0	100.0	0.0
Beach	0.2	0.1	1.7	10.3	9.7	0.6
Channel bar	0.6	0.1	0.2	73.2	68.4	0.1
Creek	4.1	1.1	5.0	44.8	40.1	0.3
Mangrove	112.9	31.2	14.1	89.9	72.7	0.3
Marsh	36.4	38.0	39.3	48.1	32.0	1.0
Channel island	1.7	0.1	0.1	94.4	88.0	0.1
Spit	2.5	0.6	0.5	83.2	68.1	0.3
Beach ridge and swale	23.7	15.0	6.7	78.0	52.2	0.6
Natural levee	1.5	0.08	0.3	81.7	78.3	0.1

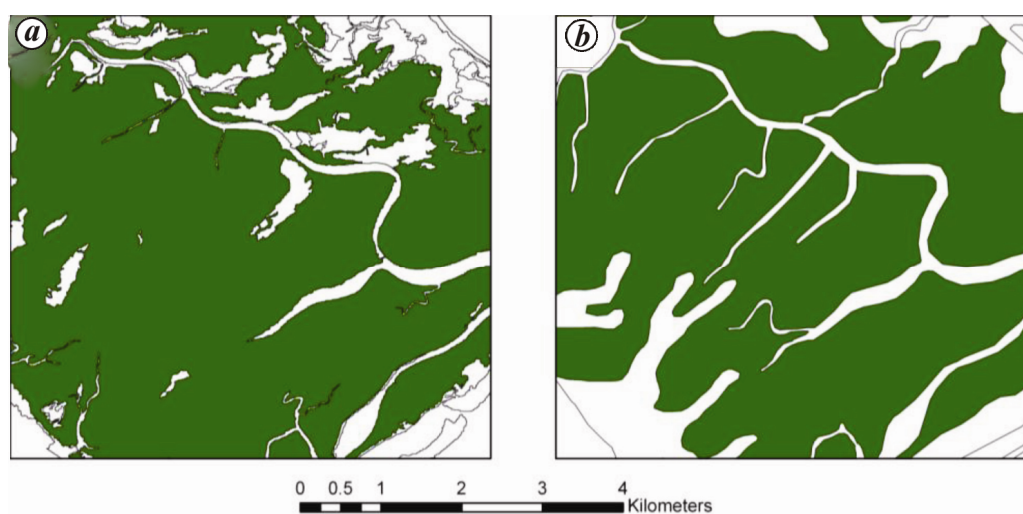


**Figure 9.** *a*, Classified map of mangrove; *b*, Reference map of mangrove.

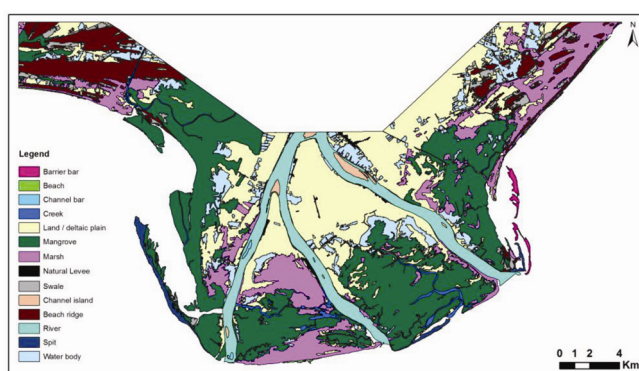


**Figure 10.** Landform map of the Krishna delta.

accuracy of few landforms was marginally less due to rampant aquaculture activities practiced by farmers in this area by modifying landforms such as beach ridges and natural levees through withdrawal of saline water from deep bore wells.

The main aim of this study was to classify coastal and fluvial landforms in a deltaic region semi-automatically by OBIA technique using a knowledge-based multi-scale

classification approach. OBIA could efficiently translate knowledge with respect to image features/objects. Eleven different types of fluvial and coastal landforms were classified using OBIA in the Krishna delta, India. Optimum scales derived using POF were able to create objects for classification of landforms of different sizes.

Coastal landforms protect the coastal areas and human life from various disasters. Mangroves have the ability to withhold the sand near the coast, which prevents soil erosion by wave action. Mangrove in this area was detected with 89.9% accuracy. Similarly, the beach ridges were effective in providing protection from the cyclonic winds and storm surges from destroying the ecosystem surrounding them. Beach ridges and swales were classified with 78% accuracy. Usage of DEM in classification of beach ridge was helpful as most of the beach ridges were altered in the area for aquaculture activity and thus offer a different spectral attribute. Similarly, classification of natural levee was possible using OBIA due to the usage of high resolution LiDAR DEM. The knowledge-based OBIA classification is generic and can be used in other deltaic areas for semi-automatic mapping of landforms.

1. SAC (ISRO), *Coastal Zones of India*, Space Applications Centre (ISRO), Ahmedabad, India, 2012; <http://sac.gov.in>
2. Nageswara Rao, K., Evolution and dynamics of the Krishna Delta, India. *Natl. Geograph. J. India*, 1985, **31**, 1–9.
3. Prabakaran, S., Srinivasa Raju, K., Lakshumanan, C. and Ramalingam, M., Remote sensing and GIS applications on change detection study in coastal zone using multi temporal satellite data. *Int. J. Geomatics Geosci.*, 2010, **1**, 2.
4. Saranathan, E., Chandrasekaran, R., Soosai Manickaraj, D. and Kannan, M., Shoreline changes in Tharangampadi village, Nagapattinam district, Tamil Nadu, India – a case study. *J. Indian Soc. Remote Sensing*, 2011, **39**, 107–115.
5. Bishop, M. P., Shroder, J. J. F. and Colby, J. D., Remote sensing and geomorphometry for studying relief production in high mountains. *Geomorphology*, 2003, **55**(1–4), 345–361.
6. Iwahashi, J. and Pike, R. J., Automated classifications of topography from DEMs by an unsupervised nested-means algorithm and a three-part geometric signature. *Geomorphology*, 2007, **86**(3–4), 409–440.
7. Smith, M. J. and Pain, C. F., Applications of remote sensing in geomorphology. *Progress Phys. Geography*, 2009, **33**(4), 568–582.
8. Gustavsson, M., Development of a detailed geomorphological mapping system and GIS geodatabase in Sweden, Digital Comprehensive Summaries of Uppsala Dissertations from the Faculty of Science and Technology, 2006, p. 236.
9. Philip, G. and Sah, M. P., Geomorphic signatures of active tectonics in the Trans-Yamuna segment of the western Doon valley, northwest Himalaya, India. *Int. J. Appl. Earth Observ. Geoinfor.*, 1999, **1**(1), 54–63.
10. Shroder Jr, J. F. and Bishop, M. P., A perspective on computer modeling and fieldwork. *Geomorphology*, 2003, **53**, 1–9.
11. Martha, T. R., Sharma, A. and Vinod Kumar, K., Development of meander cutoffs – a multi-temporal satellite-based observation in parts of Sindh River, Madhya Pradesh, India. *Arabian J. Geosci.*, 2015, **8**(8), 5663–5668.
12. Martha, T. R., Ghosh, D., Vinod Kumar, K., Lesslie, A. and Ravi Kumar, M. V., Geospatial technologies for national geomorphology and lineament mapping project – a case study of Goa state. *J. Indian Soc. Remote Sensing*, 2013, **41**, 905–920.
13. Xiaojun, Y., Damen, M. C. J. and Van Zuidam, R. A., Use of thematic mapper imagery with a geographic information system for geomorphologic mapping in a large deltaic lowland environment. *Int. J. Remote Sensing*, 1999, **20**(4), 659–681.
14. Dragut, L. and Blaschke, T., Automated classification of landform elements using object-based image analysis. *Geomorphology*, 2006, **81**(3/4), 330–344.
15. van Asselen, S. and Seijmonsbergen, A. C., Expert-driven semi-automated geomorphological mapping for a mountainous area using a laser DTM. *Geomorphology*, 2006, **78**(3–4), 309–320.
16. Schneevoigt, N. J., van der Linden, S., Thamm, H. P. and Schrott, L., Detecting Alpine landforms from remotely sensed imagery – A pilot study in the Bavarian Alps. *Geomorphology*, 2008, **93**(1–2), 104–119.
17. Dragut, L. and Eisank, C., Automated object-based classification of topography from SRTM data. *Geomorphology*, 2012, **142/141**, 21–33.
18. Hay, G. J. and Castilla, G., Object-based image analysis: Strengths, weaknesses, opportunities and threats (SWOT). In Proceedings OBIA, Commission VI, WG VI/4, Calgary, CA, 2006.
19. Myint, S. W., Gober, P., Brazel, A., Grossman-Clarke, S. and Weng, Q., Per-pixel vs object-based classification of urban land cover extraction using high spatial resolution imagery. *Remote Sensing Environ.*, 2011, **115**, 1145–1161.
20. Babu, P. V. L. P., Morphological evolution of the Krishna delta. *Photonirvachak*, 1975, **3**, 21–27.
21. Nageswara Rao, K. and Vaidyanadhan, R., Evolution of the coastal landforms in the Krishna delta front, India. *Trans. Inst. Indian Geogr.*, 1979, **1**, 25–32.
22. Gamage, N. and Smakhtin, V., Do river deltas in east India retreat? a case of the Krishna Delta. *Geomorphology*, 2009, **103**, 533–540.
23. Baatz, M. and Schäpe, A., Multiresolution Segmentation: an optimization approach for high quality multi-scale image segmentation. In *Angewandte Geographische Informationsverarbeitung XII, Beiträge zum AGIT Symposium Salzburg* (eds Strobl, L. J., Blaschke, T. and Griesebener, T.), Herbert Wichmann Verlag, Heidelberg, 2000, pp. 12–23.
24. Martha, T. R., Kerle, N., Jetten, V., van Westen, C. J. and Vinod Kumar, K., Characterizing spectral, spatial and morphometric properties of landslides for automatic detection using object-oriented methods. *Geomorphology*, 2010, **116**(1–2), 24–36.
25. Vamshi, G. T., Martha, T. R. and Vinod Kumar, K., An object-based classification method for automatic detection of lunar impact craters from topographic data. *Adv. Space Res.*, 2016, **57**, 1978–1988.
26. Martha, T. R., Kerle, N., van Westen, C. J., Jetten, V. and Vinod Kumar, K., Segment optimisation and data-driven thresholding for knowledge-based landslide detection by object-based image analysis. *IEEE Trans. Geosci. Remote Sensing*, 2011, **49**(12), 4928–4943.
27. GSI, ISRO, Manual for National Geomorphological and Lineament Mapping on 1 : 50,000 scale. A Project under National (Natural) Resources Census (NRC), 2010.
28. Shufelt, J. A., Performance evaluation and analysis of monocular building extraction from aerial imagery. *IEEE Trans. Pattern Anal. Mach. Intell.*, 1999, **21**(4), 311–326.

ACKNOWLEDGEMENTS. This paper is an outcome of the research work carried out at NRSC, Hyderabad. We acknowledge GM and AS and DMA team of NRSC for providing LiDAR data for the research work. We thank Dr Y. V. N. Krishnamurthy (Director, NRSC), Shri V. Bhanumurthy (Associate Director, NRSC) and Dr P. V. N. Rao (Deputy Director, Remote Sensing Applications Area), Dr V. K. Dadhwal (former Director, NRSC) and Dr P. G. Diwakar (former Deputy Director, Remote Sensing Applications Area, NRSC) for their support and encouragement to complete the work. A.M.V. is grateful to Dr P. Jagadeeshwara Rao (Department of Geo-Engineering at AUCE (A)), Visakhapatnam for help in carrying out the project work at NRSC, Hyderabad.

Received 28 February 2017; revised accepted 5 September 2017

doi: 10.18520/cs/v114/i06/1338-1345